

## Long Sustainment of Quasi-steady State High $\beta_p$ H-mode Discharges in JT-60U

A. Isayama, Y. Kamada, T. Ozeki, S. Ide, T. Fujita, T. Oikawa, T. Suzuki, Y. Neyatani, N. Isei, K. Hamamatsu, Y. Ikeda, K. Takahashi, K. Kajiwara and the JT-60 Team

Japan Atomic Energy Research Institute, Naka Fusion Research Establishment,  
Naka-machi, Naka-gun, Ibaraki-ken, 311-0193, Japan

e-mail contact of main author: isayama@naka.jaeri.go.jp

**Abstract:** Quasi-steady state high  $\beta_p$  H-mode discharges performed by suppressing neoclassical tearing modes (NTM) is described. Two operational scenarios have been developed for long sustainment of the high  $\beta_p$  H-mode discharge: NTM suppression by profile optimization and NTM stabilization by local electron cyclotron current drive (ECCD) / electron cyclotron heating (ECH) at the magnetic island. By optimizing pressure and safety factor profiles, a high  $\beta_p$  H-mode plasma with  $H_{89PL}=2.8$ ,  $HHy2=1.4$ ,  $\beta_p=2.0$ ,  $\beta_N=2.5$  has been sustained for 1.3 s at small values of  $v_{e^*}$  and  $\rho_{i^*}$ . without destabilizing the NTMs. Characteristics of the NTMs destabilized in the region of the central safety factor above unity are investigated. Relation between the beta value at the mode onset  $\beta_N^{on}$  and that at the mode disappearance  $\beta_N^{off}$  can be described as  $\beta_N^{off}=0.05-0.4 \beta_N^{on}$ , which shows the existence of hysteresis. The value of  $\beta_N/\rho_{i^*}$  at the onset of an  $m/n=3/2$  NTM has collisionality dependence, which is empirically given by  $\beta_N/\rho_{i^*} \propto v_{e^*}^{0.36}$ . However, the profile effects are equally important, such as relative shapes of pressure and safety factor. Onset condition seems to be affected by strength of the pressure gradient at the mode rational surface. Stabilization of the NTM by local ECCD/ECH at the magnetic island has been attempted. The  $3/2$  NTM has been completely stabilized by EC wave injection of 1.6 MW.

### 1. Introduction

The quasi-steady state high  $\beta_p$  H-mode discharges is characterized by a monotonic safety factor profile with the central safety factor  $q(0)$  above unity and the internal transport barrier produced at a weak positive magnetic shear. Achievable beta and duration have been steadily improved by increasing the edge pressure by increasing triangularity [1], optimizing global pressure profiles for both the edge stability limit determined by ELMs and the central stability limit determined by the kink-ballooning mode [2] and optimizing edge stability by accessing to the second stability regime [3]. However, even after the stabilization of these ideal instabilities, we found that achievable beta and duration of the quasi-steady state high  $\beta_p$  H-mode discharge are still limited by low-n resistive MHD instabilities [2]. We found that these instabilities are characterized by the magnetic island growing with increasing the beta value and can be attributed to the neoclassical tearing modes (NTMs) [4, 5]. Two operational scenarios have been applied to suppress the NTMs: avoidance of destabilization of the NTMs by profile optimization and stabilization of the NTM by local electron cyclotron current drive (ECCD) / electron cyclotron heating (ECH) at the magnetic island. In this paper, sustainment of the quasi-steady state high  $\beta_p$  H-mode discharges performed by suppressing the NTMs is described.

### 2. Sustainment of the Quasi-steady State High $\beta_p$ H-mode Plasmas

JT-60U has been optimizing the operational scheme for the quasi-steady state high  $\beta_p$  H-mode discharge aiming at long sustainment of 1) high confinement and high beta, 2) large fraction of non-inductive driven current, 3) high efficiency of particle exhaust. Figure 1 demonstrates the recently achieved product of the normalized beta and H-factor,  $\beta_N H_{89PL}$ , versus duration in this regime.  $\beta_N H_{89PL} \approx 7$  has been sustained for 1.3 s ( $\approx 3\tau_E$ ) with full noninductive current drive, and  $\beta_N H_{89PL} \approx 5.5$  has been sustained for 2.8 s ( $\approx 12\tau_E$ ) at  $q_{95}=3.3$ .

Typical waveforms are shown in Fig. 2. Plasma parameters are as follows: plasma current  $I_p=1.5$  MA, toroidal magnetic field  $B_t=3.74$  T, major radius  $R=3.22$  m, minor radius  $a=0.79$  m, elongation  $\epsilon=1.54$ , triangularity  $\delta=0.35$ , safety factor at the 95% flux surface  $q_{95}=4.7$ . By using positive-ion-based neutral beams (P-NBs) of 20 MW, negative-ion-based neutral beams (N-NBs) of 4.1 MW and on-axis ECH of 1.6 MW, a high  $\beta_p$  H-mode plasma with  $\beta_p \approx 2.0$  and  $\beta_N \approx 2.5$  has been sustained for 1.3 s. Loop voltage (Fig. 2(d)) is kept around zero, which shows that the full non-inductive current drive condition is satisfied. In this discharge, confinement enhancement factor over the L-mode scaling  $H_{89PL}$  is 2.9, and that over the ELMY H-mode scaling  $HHy2$  is 1.4. In this discharge, current drive efficiency of

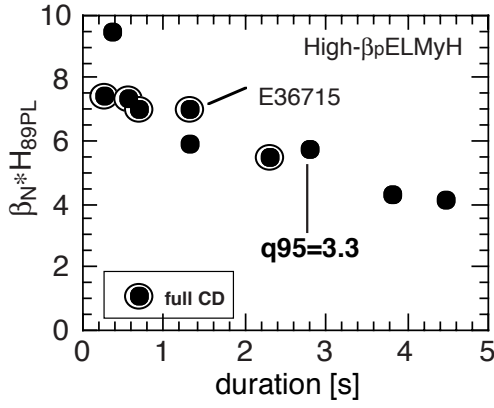


FIG. 1.  $\beta_N H_{89PL}$  versus duration obtained in the high  $\beta_p$  H-mode discharges.

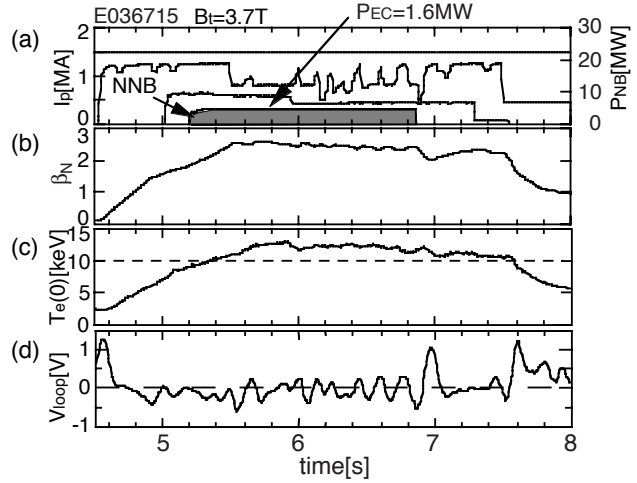


FIG. 2. Typical waveforms of the high  $\beta_p$  H-mode discharge.

$1.55 \times 10^{19}$  Am<sup>-2</sup>W<sup>-1</sup> is achieved simultaneously [6]. Thus, this discharge is consistent from the viewpoint of current drive as well as confinement and beta. Note that at least no detectable NTM is observed throughout the discharge even at low collisionality of  $v_{e^*} \approx 0.005$ . The detail of the NTM is discussed in the subsequent sections.

### 3. Characteristics of Neoclassical Tearing Modes in the High $\beta_p$ H-mode Discharges

Sustainable beta and duration of the quasi-steady state high  $\beta_p$  H-mode discharges are limited by low- $n$  ( $n=1-3$ ) tearing modes such as  $m/n=3/2$  and  $2/1$  modes. Here,  $m$  and  $n$  are poloidal and toroidal mode numbers, respectively. From this series of discharges, the tearing modes are considered to be the NTMs [4, 5]. The NTM in JT-60U is distinctive in that they appear in  $q(0) > 1$  region. Characteristics of the NTM in this region have been investigated.

First, we investigate the hysteresis in the beta value at which the NTM appears  $\beta_N^{on}$  and that at which the NTM disappears  $\beta_N^{off}$ . Time evolutions of the normalized beta after NB injection are shown in Fig. 3(a). In shot E36855, the  $3/2$  mode appears at 5.7 s when  $\beta_N$  reaches 1.6, while no NTM is observed throughout the discharge in shot E36854 where  $\beta_N$  is sustained at 1.4. Thus, the onset  $\beta_N$  in these discharge region ( $I_p=1.5$ MA,  $B_T=3.6$ T) is in the range of 1.4 - 1.6. Figure 3(b) shows time evolutions of  $\beta_N$  after the step-down of NB power. In shot E36882, the  $3/2$  mode disappears at  $t \approx 6.8$  s when  $\beta_N$  decreases to 0.5. In shot E36896, where  $\beta_N$  is kept at 0.7, the  $3/2$  mode persists until turn-off of the NB power ( $t > 10$  s). Thus,

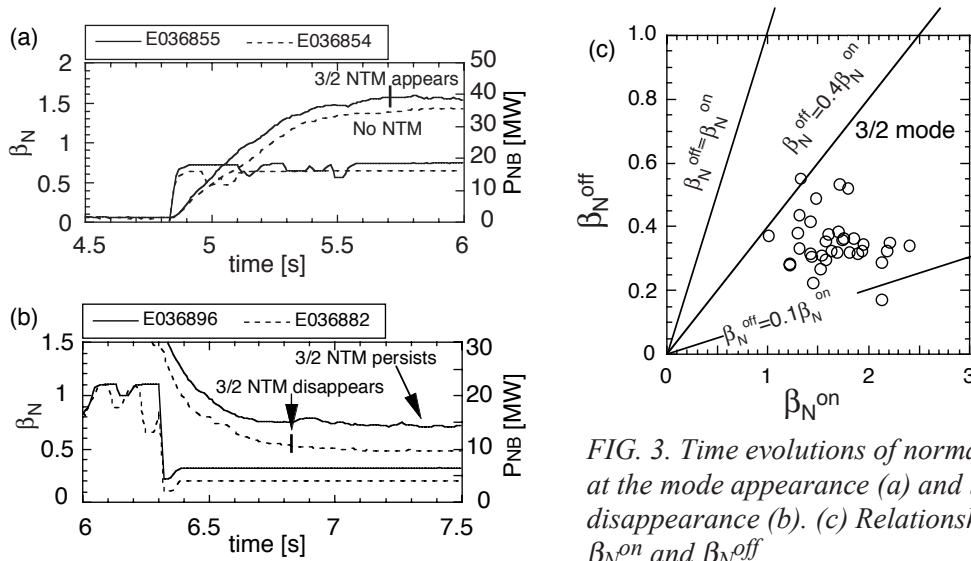


FIG. 3. Time evolutions of normalized beta at the mode appearance (a) and the mode disappearance (b). (c) Relationship between  $\beta_N^{on}$  and  $\beta_N^{off}$

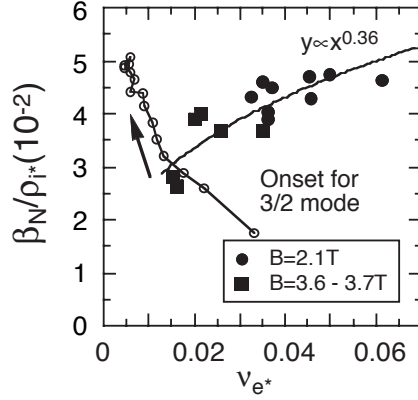


FIG. 4. Dependence of onset  $\beta_N$  normalized by Larmor radius on collisionality. Open circles correspond to the discharge shown in Fig. 2, where no NTM is observed.

$\beta_N$  at which the NTM disappears is in the range of 0.5 - 0.7. These results show the existence of hysteresis in  $\beta_N^{\text{on}}$  and  $\beta_N^{\text{off}}$ , which can be described as  $\beta_N^{\text{off}} \approx 0.3 \beta_N^{\text{on}}$ . Fig. 3(c) shows the relation between  $\beta_N^{\text{on}}$  and  $\beta_N^{\text{off}}$  under various discharge conditions. The observed hysteresis is described as  $\beta_N^{\text{off}} \approx 0.05 - 0.4 \beta_N^{\text{on}}$ .

Collisionality dependence of onset  $\beta_N$  for a 3/2 mode is shown in Fig. 4, where  $\beta_N$  normalized by toroidal ion Larmor radius  $\rho_{i^*}$  is plotted versus  $\nu_{e^*}$ . In this plot, parameters at  $\rho=0.5$ , which correspond to those at the mode rational surface, are used for evaluation of  $\rho_{i^*}$  and  $\nu_{e^*}$ . Closed circles and closed squares correspond to the discharges in the regions of  $I_p=1.0$  MA /  $B_t=2.1$  T ( $q_{95}=3.4-3.7$ ) and  $I_p=1.5$  MA /  $B_t=3.6 - 3.7$  T ( $q_{95}=4.0 - 4.4$ ), respectively. As shown in this figure, value of  $\beta_N/\rho_{i^*}$  has a positive dependence on collisionality given by  $\beta_N/\rho_{i^*} \propto \nu_{e^*}^{0.36}$ .

#### 4. Effects of Profiles on Neoclassical Tearing Modes

Time trace of  $\beta_N/\rho_{i^*}$  versus  $\nu_{e^*}$  in shot E36715 (Fig. 2) is also plotted in Fig. 4. In this discharge, no detectable NTM is observed throughout the discharge even though  $\nu_{e^*}$  decreases to 0.005 and  $\beta_N/\rho_{i^*}(10^{-2})$  reaches about 6, which suggests that some other factors are needed for precise description of the onset condition. We have investigated the relationship between pressure and safety factor profiles. Figure 5 compares shot E36715 with the discharge without N-NB injection (E36706). In these two discharges, the discharge condition is the same except NB injection pattern. Time traces of  $\beta_N$  and neutron emission rate in shot E36715 and E36706 are shown in Figs. 5(b) and 5(c), respectively. In shot E36706, a large 2/1 mode appears at  $t = 5.7$  s, and both the normalized beta and neutron emission rate decrease. In shot E36715, no NTM is observed even though the beta value is higher than that in shot E36706. Thermal pressure gradient profiles calculated by the ACCOME code and safety factor profiles measured by the motional Stark effect (MSE) diagnostics in these discharges are shown in Fig. 6. Safety factor is almost identical, and the

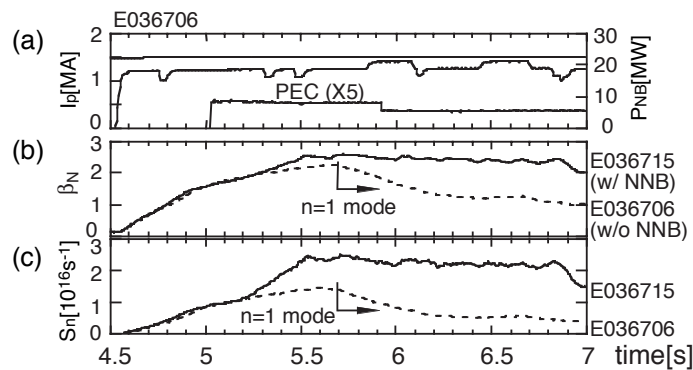


FIG. 5. Waveforms of (a) plasma current, NB power and EC power, (b) normalized beta and (c) neutron emission rate.

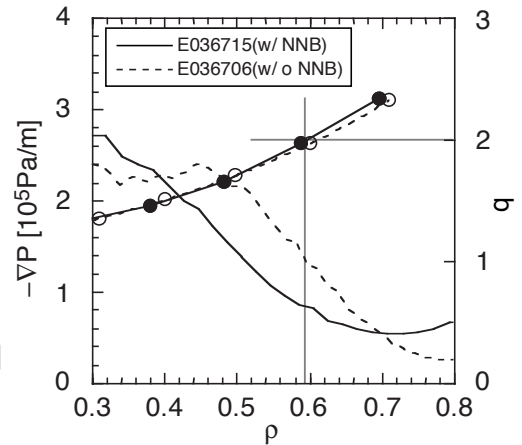


FIG. 6. Profiles of pressure gradient and safety factor in shot E36715 and E36706.

mode rational surface for the 2/1 mode is located at  $\rho \approx 0.6$  in both cases. Collisionality and Larmor radius are also similar in these discharges ( $\nu_e \approx 0.01$ ,  $\rho_i \approx 0.005$ ). Only one notable difference is observed in the pressure gradient profiles: the pressure gradients at the  $q=2$  surface in shots E36715 (w/o NTM) and E36706 (with NTM) are  $0.8 \times 10^5$  Pa/m and  $1.3 \times 10^5$  Pa/m, respectively. This difference is caused by the difference in heating profiles of P-NB and N-NB. Since the heating profile of N-NB is more center-peaked one, the pressure profile also becomes peaked, which reduces the pressure gradient near the  $q=2$  rational surface ( $\rho \approx 0.6$ ). This result shows that reduction of the pressure gradient at the mode rational surface improves the stability for the NTMs. The result does not directly show the difference in bootstrap current profiles because the current profile does not reach a steady state (especially shot E36706), but the result implies that in shot E36715 the 2/1 NTM is suppressed by modification of bootstrap current profile at the  $q=2$  surface.

### 5. Stabilization of 3/2 Neoclassical Tearing Mode by ECCD/ECH at the Magnetic Island

After installation of the 110 GHz EC wave injection system [7] in JT-60U, experiments on the tearing mode stabilization by local current drive and heating at the magnetic island using the first harmonic EC wave have been performed [5]. The shape of plasma cross section is shown in Fig. 7(a). The EC wave is obliquely injected from the low field side with the toroidal injection angle of about  $20^\circ$ .

For current drive and heating just at the magnetic island, we need to identify the mode location with high accuracy. We have precisely identified the mode location using the electron cyclotron emission (ECE) heterodyne radiometer. Amplitude and phase of electron temperature perturbations just before ECCD/ECH are shown in Fig. 7(b). Decrease in amplitude and jump in phase are observed across  $R=3.67$  m, which suggests that the center of the island is located at this position. Safety factor profile measured by the MSE diagnostics shows that the  $q=1.5$  surface is located at this position. Mode location was also identified by scanning the steerable mirror angle during a discharge as shown in Fig. 8, where the steerable mirror angle is changed from  $40^\circ$  to  $44.5^\circ$ , which corresponds to shift of EC resonant location from  $\rho \approx 0.7$  to  $0.4$ . When the angle is  $43^\circ$  at  $t=9.5$  s, which corresponds to deposition at  $\rho \approx 0.5$ , the amplitude of the magnetic perturbations with  $n=2$  (Fig. 8(b)) starts to decrease. The optimum injection angle determined by this method agrees with that obtained by ECE and MSE diagnostics.

Time evolution of magnetic perturbations with  $n=2$  during ECCD/ECH is shown in Fig. 9. In this discharge, injection angle is set at  $43^\circ$ . Amplitude of the magnetic perturbations begins to decrease after the unmodulated EC wave injection at 7.52 s, and completely stabilized at

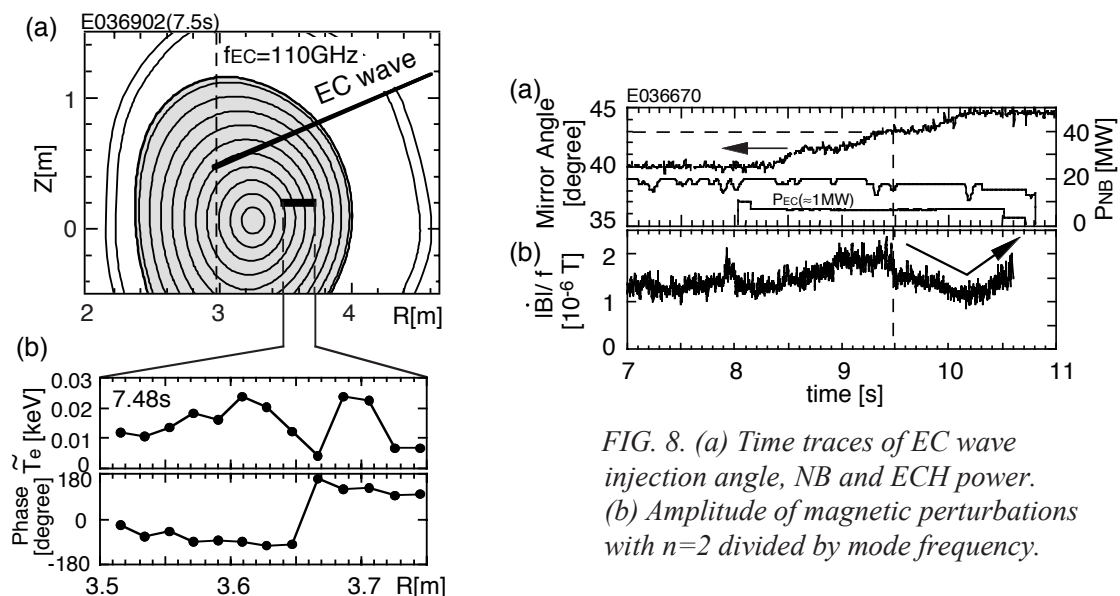


FIG 7. (a) Plasma cross section and rays of injected EC wave. (b) Amplitude and phase of electron temperature perturbations.

FIG. 8. (a) Time traces of EC wave injection angle, NB and ECH power. (b) Amplitude of magnetic perturbations with  $n=2$  divided by mode frequency.

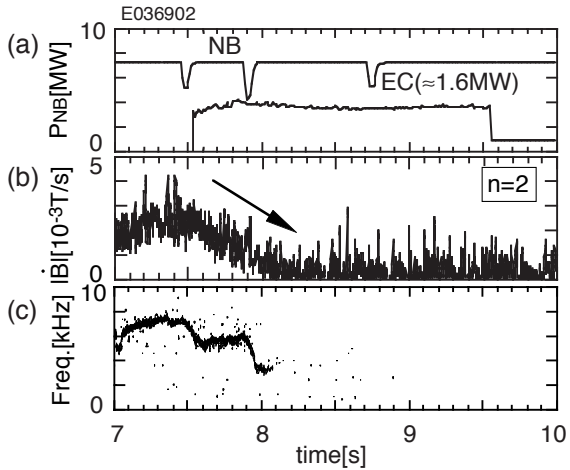


FIG. 9. (a) Time traces of NB and ECH power. (b) Amplitude of magnetic perturbations with  $n=2$ . (c) Frequency of the perturbations.

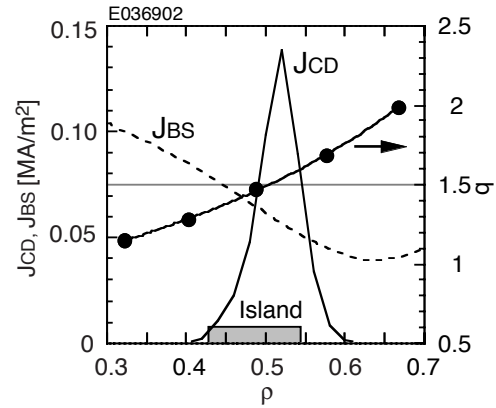


FIG. 10. Profiles of EC driven current, bootstrap current and safety factor. Shaded region corresponds to the location of the magnetic island estimated from the  $T_e$  perturbation profile in Fig. 7(b).

$t=8.2$  s. Without EC wave injection, the  $3/2$  mode persists throughout the NB phase. In this discharge, NB power, ECH power are 7.5 MW and 1.6 MW, respectively. Ohmic heating power is calculated to be 0.4 MW using the transport analysis code (TOPICS). Thus, ratio of the ECH power to the total heating power is 17%. The EC driven current calculated by a Fokker-Planck code is about 25 kA, which is 2% of the total plasma current of 1.5 MA. EC driven current profile calculated by the Fokker-Planck code and bootstrap current profile calculated by the ACCOME code are shown in Fig. 10. Maximum EC driven current density is about 1.5 - 2 times larger than that of the bootstrap current density. The width of the EC driven current profile is comparable to the magnetic island width evaluated from the electron temperature perturbation profile in Fig. 7(b). Safety factor profile measured by the MSE diagnostics shows that the injected EC wave is deposited at the  $q=1.5$  surface.

So far, complete stabilization is achieved in the low beta region ( $\beta_N \approx 0.8$ ). In higher beta region, only partial stabilization, shrinkage of magnetic island, has been observed since available EC power is small. Complete stabilization of the NTM in the higher beta region will be attempted with higher EC wave injection power in 2001.

## 6. Conclusions

The high  $\beta_p$  H-mode plasma with  $H_{89PL}=2.8$ ,  $H_{H_{y2}}=1.4$ ,  $\beta_p \approx 2.0$ ,  $\beta_N \approx 2.5$  have been sustained for 1.3 s with suppression of the NTMs by profile optimization. Characteristics of the NTMs destabilized in the  $q(0) > 1$  region are investigated. Hysteresis exists in the beta value at the mode onset  $\beta_N^{\text{on}}$  and that at the mode disappearance  $\beta_N^{\text{off}}$ , which is described as  $\beta_N^{\text{off}} = 0.05 - 0.4 \beta_N^{\text{on}}$ . The value of  $\beta_N / \rho_{i*}$  at the onset of a  $3/2$  NTM has a collisionality dependence of  $\beta_N / \rho_{i*} \propto \nu_e^{*0.36}$ . Onset condition seems to be affected by strength of the pressure gradient at the mode rational surface. Stabilization of the NTM by ECCD/ECH at the magnetic island has been attempted. A  $3/2$  NTM has been completely stabilized with the EC wave power of 1.6 MW, 17% of the total heating power, and EC driven current of 25 kA, 2% of the total plasma current.

## References

- [1] KAMADA, Y., et al., Proc. 15th Int. Conf. Fusion Energy, Seville 1994 (IAEA, Vienna, 1995) vol 1, p 651.
- [2] KAMADA, Y., et al., Proc. 16th Int. Conf. Fusion Energy, Montreal (IAEA, Vienna, 1997) vol 1, p 247.
- [3] KAMADA, Y., et al., Nucl. Fusion **39** (1999) 1845.
- [4] ISAYAMA, A., et al., Plasma Phys. Control. Fusion **41**(1999) 35.
- [5] ISAYAMA, A., et al., to be published in Journal of Plasma and Fusion Research.
- [6] OIKAWA, T., et al., IAEA-CN-77/EX8/3, this conference.
- [7] IKEDA, Y., et al., IAEA-CN-77/EXP4/03, this conference.